Revista de Ensino de Ciências e Matemática
ONLINE ISSN 2178-7727

Performance, Combustion and Emission analysis of Jatropha oil of Biodiesel engine with nano additives: an Experimental Study

C R Raghavendra[a], Vinay S S[b], Sriharsha A M[c], Kumara B M[d*], Kishan Naik[e], Anjaneya G[f]

[a,d] Department of Mechanical Engineering, Government Engineering College, Haveri, Karnataka, India

[b,c] Department of Mechanical Engineering, Government Engineering College, Mosalehosalli, Hassan, Karnataka, India

[e] Department of Mechanical Engineering, University BDT College of Engineering, Davanagere, Karnataka, India

[f] Department of Mechanical Engineering, R V College of Engineering, Bengaluru, Karnataka, India

*Corresponding author mail: kumarvanitha80@gmail.com

Submitted:** 30 Jan. 2023. **Accepted:** 26 Jul. 2023. **Publication:** 01 Aug.2023*

ABSTRACT

The fast depletion of crude oil reserves and the resultant environmental damage drive the pressing search for alternative fuel sources for internal combustion engines. Biodiesel stands out as a promising candidate for compression ignition engines due to its advantageous heat content and combustion qualities. Utilized across various vehicles and equipment such as cars, trucks, buses, off-road vehicles, and oil furnaces, blends of Biodiesel present substantial potential for emission reduction, up to 76% from Biodiesel engines, alongside improving engine lifespan thanks to their superior lubrication properties. Nevertheless, biodiesel comes with certain drawbacks, including reduced performance and increased nitrogen oxide emissions. Hence, the focus of this study is to investigate the utilization of locally available biodiesel in a low-heat rejection engine, complemented by nano additives, aiming to improve performance while

reducing nitrogen oxide emissions. India currently boasts numerous biodiesel sources, ranging from vegetable oil to Jatropha oil, which can be effectively utilized in biodiesel engines by incorporating fatty acid ester and glycerol. The experimental setup involves a single-cylinder 4-stroke water-cooled biodiesel engine producing 5.2 kW of power. An installed water-cooled piezoelectric pickup, ranging from 0 to 250 bar, was utilized on the cylinder head for engine cylinder pressure measurement. The optical crank angle (CA) encoder (Manufacturer: Kistler, Model: Type 2613B) was employed to determine crankshaft position, enabling the measurement of cylinder pressure at different crank angles. Both coated and uncoated engines underwent testing with varying proportions of Jatropha oil. The results reveal a significant improvement in engine performance across all loads compared to the baseline engine. Additionally, when combined with L-ascorbic acid, these biodiesels exhibit a noticeable decrease in nitrogen oxide emissions.

Keywords: *Biodiesel Engine, Jatropha oil, nitrogen oxide emissions*

1. Introduction

In the experimental setup, a single-cylinder 4-stroke water-cooled biodiesel engine generating 5.2 kW of power was employed. Engine cylinder pressure was monitored using a water-cooled piezoelectric pickup, capable of measuring within a range of 0 to 250 bar, attached to the cylinder head. Crankshaft position was determined by utilizing an optical crank angle (CA) encoder (Manufacturer: Kistler, Model: Type 2613B) to measure cylinder pressure at various crank angles. Experiments were carried out on both coated and uncoated engines utilizing various blends of Jatropha oil. The conclusive findings demonstrate a significant enhancement in engine performance across all operational parameters compared to the conventional engine setup. Additionally, the inclusion of L-ascorbic acid with these biodiesels results in a notable reduction in nitrogen oxide emissions.

The production process utilized esterification/transesterification techniques. When refined oil is used as the feedstock, the need for multiple processing stages constitutes over 70% of the total production costs of biodiesel. Therefore, implementing a combined process that integrates extraction, esterification, and transesterification, known as reactive extraction, shows potential for lowering processing costs. Reactive-extraction diverges from the conventional method of biodiesel production, where the oil-bearing material directly interacts with alcohol instead of reacting with pre-extracted oil. Essentially, extraction and transesterification happen concurrently, with alcohol serving as both an extraction solvent and a transesterification reagent. Since its introduction by Harrington and D'arcy Evans, numerous researchers have examined the effectiveness and feasibility of this approach. However, the possibility of substituting current transesterification methods with reactive-extraction remains ambiguous. The successful

implementation of biodiesel production via reactive-extraction depends on a thorough understanding and characterization of the entire process. Various parameters play a role in the reactive extraction of oil-bearing biomass for biodiesel production. Furthermore, Haas et al. emphasized that biodiesel obtained through reactive-extraction often involves higher expenses compared to biodiesel produced using traditional transesterification, primarily due to the significant amounts of methanol required for the process. The integration of reactive-extraction not only simplifies the process but also eliminates the need for a dedicated step to extract hazardous substances during subsequent processing stages, thus reducing workers' exposure to such compounds. This approach, however, can be applied to almost any lipid-containing material. Numerous studies have documented the use of an incubator shaker in biochemical and biocatalytic reactions. Esterification reactions involving 4-methyloctanoic acid (4-MOA) with PEG in an organic monophase and water/organic biphasic system, utilizing Novozym435 R as the catalyst, were conducted in a New Brunswick Scientific Innova TM 4080 incubator shaker operating at 350 rpm and 45°C. Similarly, enzymatic transesterification was carried out to convert racemic 4-methyl hexanoic acid methyl ester and 4-methyloctanoic methyl ester into their respective butyl esters, using a New Brunswick Scientific Innova TM 4080 incubator shaker. Additionally, significant research has investigated the extraction of algae oil followed by its transesterification, conducted in an electric shaker at 300 rpm for 3 hours. The present study aims to assess the influence of various crucial parameters on the reactive extraction of Jatropha seeds for biodiesel production, utilizing an incubator shaker in the author's research laboratory, as depicted in the figure.

Figure 1: Four stroke diesel engine setup in Lab

The objective of the research is to extract biodiesel from Jatropha oil using transesterification. Subsequently, a blend called B40 is created by blending conventional diesel with Jatropha biodiesel and nano additives. The optimization of engine operating conditions, including load, compression ratio, and injection pressure, is undertaken to enhance performance parameters and reduce emission levels while utilizing various proportions of biodiesel and additives. Experimental analysis of the B40 blend, combined with various nano additives like Al_2O_3, SiO_2,

and TiO_2, is performed under different loads and injection pressures. Furthermore, the impact of injection pressure of the B40 blend diesel, augmented with nano additives, under different loads applied to the engines, is examined. The study also investigates the performance and attributes of engines using B40 biodiesel with nano additives, emphasizing combustion, emissions, and performance metrics such as brake thermal efficiency and specific fuel combustion. Additionally, exhaust gas temperature and smoke analysis emission tests are carried out for NO_X and CO_x analysis.

2. Experimental Methodologies

The current study involves the establishment of a transesterification process setup and an experimental test rig for a compression ignition (CI) engine. Consequently, an experimental setup was constructed, equipped with essential instrumentation, to assess the performance, emissions, and combustion parameters of the CI engine under various operating conditions. Crude vegetable oils exhibit high viscosity and are deemed undesirable. Hence, it is imperative to reduce viscosity and separate the glycerin content from vegetable oil. Transesterification of vegetable oil is thus deemed more suitable for all types of vegetable oils. This section elaborates on the details of the transesterification setup, experimental arrangement, instruments utilized, and the development of specific components and software necessary for the research.

2.2. Jatropha oil

Millettia pinnata, commonly known as P. pinnata, is an evergreen tree abundant in the rainforests of Asia, particularly in the Jatropha region. The tree typically starts bearing pods around its fifth year of growth, with pod production gradually increasing until stabilizing around the twelfth year. Jatropha oil, derived from the seeds, can be obtained through mechanical expeller, cold pressing, or solvent extraction methods, yielding an oil with a yellowish-orange to brown coloration.

Figure 2: Jatropha **pod and seed.**

3.1 Transesterification

The transesterification setup comprises a 2-liter capacity round-bottom flask with three necks, placed in a water bath for heating the oil [see Fig. 1]. Heating of the oil in the round-bottom flask was facilitated by a heater equipped with a temperature regulator. Mixing of the oil was achieved using a high-speed motor with a magnetic stirrer, functioning as a rotating element, to ensure vigorous mixing. During the transesterification process, triglycerides from Honge oil react with methyl alcohol in the presence of a catalyst (NAOH/KOH) to yield fatty acid esters and glycerol. For this process, 1000 grams of Honge oil, 240 grams of methanol, and 8 grams of sodium hydroxide were introduced into the round-bottom flask. Figure 2 displays the essential items needed for the transesterification process, including Methanol, Sodium hydroxide, Sodium Sulfate, and Silica gel containers. All components were heated to 70°C and vigorously stirred by the magnetic stirrer for one hour until ester formation commenced. The mixture was then transferred to a separating funnel and left to settle overnight under gravity. The upper layer in the separating funnel, comprising the ester, was separated from the lower layer containing glycerol [see Fig. 3]. The isolated ester was combined with 250 grams of hot water and left to settle under gravity for 24 hours. Water washing was conducted to eliminate fatty acids and dissolved catalyst present in the lower layer, which was subsequently separated. Fatty acids and dissolved catalyst were further removed using a separation funnel. Silica gel crystals were then introduced to extract moisture from the ester [refer to Fig. 4].

Figure 3: Equipment for Transesterification

Figure 4: Methanol, Sodium hydroxide, Sodium Sulfate and Silica gel containers

Figure 5: Separation of JOME and Glycerin

Figure 6: Washing and moisture removal from JOME

3.2 Properties of Test Fuels (after Transesterification)

Figure 7 depicts the flow diagram for biodiesel production, while Table 1 presents the physical properties of diesel, as well as nano additives including TiO_2, SiO_2, and Al_2O_3 (100%), alongside Jatropha oil methyl ester (100%). These fuel properties are evaluated using ASTM D 6751, a standardized method for assessing fuel properties. The density of Jatropha oil with nano additives like TiO_2, SiO_2, and Al_2O_3 surpasses the EN14214 limit of 0.86−0.9, whereas the densities of other biodiesels remain within the prescribed limits, closely resembling that of diesel. Furthermore, the kinematic viscosity of nano additives like TiO_2, SiO_2, and Al_2O_3 is lower compared to other biodiesels and is much closer to that of Biodiesel. The cetane numbers of all biodiesels exceed those of diesel, indicating a higher self-ignition temperature. Table 1 provides a comparison of the properties of Biodiesel, TiO_2 (20%), SiO_2, Al_2O_3 (20%), and Jatropha oil (20%). The examination of both 20% and 100% biodiesel blends in this study can be attributed to several factors.

The viability of these blends is of utmost importance. A 20% biodiesel blend, referred to as B20, is widely adopted in many regions and readily available in the market. Extensive testing has confirmed its efficient performance in conventional diesel engines, often without requiring substantial modifications. By examining the performance and emission traits of B20, researchers can obtain valuable insights into its real-world application and evaluate its potential as a feasible alternative fuel. Moreover, regulatory mandates might shape the selection of these particular blends. In various nations or areas, standards or regulations might necessitate the use of a minimum biodiesel blend, like B20, for specific applications or to meet particular emission reduction objectives. Hence, conducting research on B20 allows researchers to assess compliance with these regulations and understand the impact of such blends on engine performance and emissions. Conversely, investigating the use of 100% biodiesel (B40) is crucial

for thoroughly assessing biodiesel's viability as a standalone fuel. This enables researchers to assess the performance and emission traits solely with biodiesel, without the inclusion of any petroleum-based diesel fuel. Acquiring insights into the behavior of B40 unveils the maximum potential of biodiesel as a sustainable and renewable fuel source for diesel engines. Covering a range of biodiesel concentrations, spanning from 20% to 100% blends, this study facilitates a thorough evaluation of their influence on engine performance, emissions, and adherence to regulatory standards.

Table 1: Properties of fuels used

Properties	Diesel	JATROPA	JOME	B20	B40	B40$Al_2O_3$80	B40$SiO_2$80	B40$TiO_2$80
Chemical Formula	$C_{13}H_{24}$	----	----	----	----	----		
Density (kg/m^3)	840	927	870	855	856	873	866	857
Calorific value (kJ/kg)	43,000	35,800	38,450	42,212	39,800	40,376	40,178	40,558
Viscosity (cSt)	2.5	5.6	5.5	4.12	3.99	4.22	4.21	4.18
Flashpoint (^oC)	75	187	170	104	108	113	136	148
Cetane Number	45-55	40	44	----	----	----		
Carbon Residue (%)	0.1	0.66	----	----	----	----		

4. Experimental Setup

Load testing was performed using a single-cylinder CI engine linked to an eddy current dynamometer for load adjustment. Load measurement was facilitated by a load cell attached to the dynamometer arm. This setup enables the measurement of both fuel flow rate and air flow rate into the engine, with provisions for monitoring and controlling the coolant flow rate. Crank angle encoder technology was utilized to determine piston position, while a PCB piezo electronics pressure transducer was employed to measure in-cylinder gas pressure.

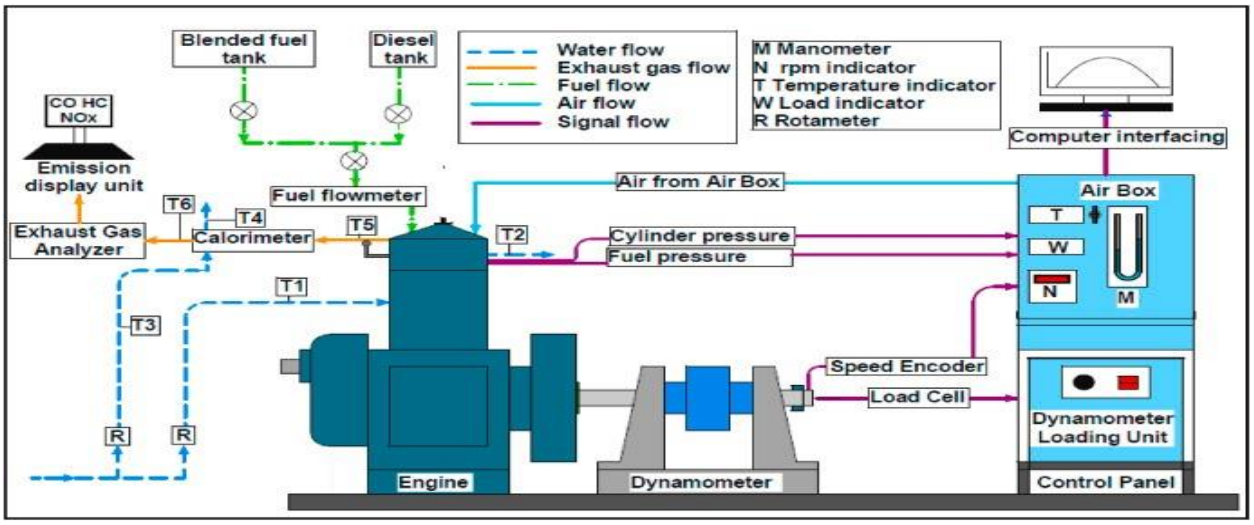

Figure 7: Photographic view of the experimental setup.

The AVL 444 digas analyzer and AVL smoke meter are employed for measuring engine exhaust emissions. The experimental setup, inclusive of all required equipment, is illustrated in Figure 7. The engine is capable of running with neat diesel at a constant speed of 1500 rpm to attain a steady-state condition. Both the exhaust gas analyzer and smoke meter are activated well in advance to ensure the stabilization of all systems before the start of the experiment.

EXPERIMENTAL SETUP

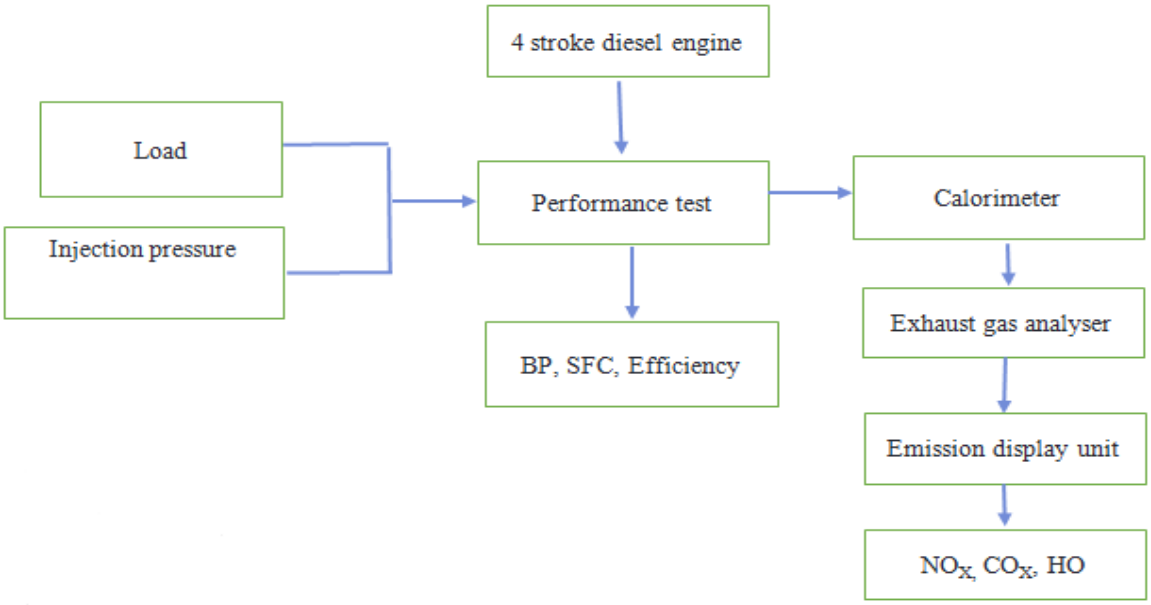

The above experimental procedure is followed for conducting all experiments. The details of the experiments for the present investigation are as follows:

1. After completing the experiments with neat diesel, the same experimental procedure is repeated with a B20 blend of the Jatropha oil with three nano additives such as TiO_2, SiO_2, and Al_2O_3. The experiments and similar observations are repeated with the B40 for TiO_2, SiO_2, and Al_2O_3. After completing the experiment with the said additives Biodiesel, the engine is allowed to run for about half an hour with Biodiesel to eliminate interference from the previous Biodiesel fuel.
2. The experiments for nano additives and Jatropha oil for 20 and 100% proportions are conducted similarly.
3. The experiment for B20 and B40 of nano additives and Jatropha oil in a lanthanum oxide- is conducted.
4. Different proportions of LA were added with Biodiesel, and experiments were conducted in a conventional engine to find the optimum proportion of LA.
5. Experiments are conducted with different proportions of LA with B20 and B40 of three Biodiesel blends in conventional engines.

5. Results and Discussion

5.1. Diesel blends with Jatropha oil and nano additives

Experiments were conducted on biodiesels and Jatropha oil with nano additives at proportions of 20% and 100%. These experiments were carried out in a single-cylinder DI engine operating at a constant speed of 1500 rpm. Observations were made regarding fuel consumption, exhaust gas

temperature (EGT), and emission parameters, including carbon monoxide (CO), hydrocarbons (HC), nitrogen oxides (NOx), and smoke. Based on these observations, brake-specific fuel consumption (BSFC) and brake thermal efficiency (BTE) were calculated, and graphs were plotted to illustrate BSFC, BTE, CO, HC, NOx, smoke, and EGT with engine brake power. A comprehensive analysis of the results and discussions on individual parameters are provided below.

5.1.1. Different Biodiesel with 20 and 100% Proportions. Experiments were conducted using proportions of 20% and 100% of nano additives, and various parameters including fuel consumption time, exhaust gas temperature (EGT), carbon monoxide (CO), hydrocarbons (HC), nitrogen oxides (NOx), and smoke emissions were observed. Graphs were generated to illustrate the variations in brake-specific fuel consumption (BSFC), brake thermal efficiency (BTE), EGT, CO emissions, HC emissions, NOx emissions, and smoke emissions in relation to brake power (BP).

5.1.1.1. Brake-Specific Fuel Consumption. Figure 8 illustrates the deviation of brake-specific fuel consumption (BSFC) relative to brake power (BP) for B40TiO_2 and 100% proportions of 200 bar TiO_2, alongside diesel. It can be observed that various biodiesel proportions exhibit higher BSFC compared to diesel.

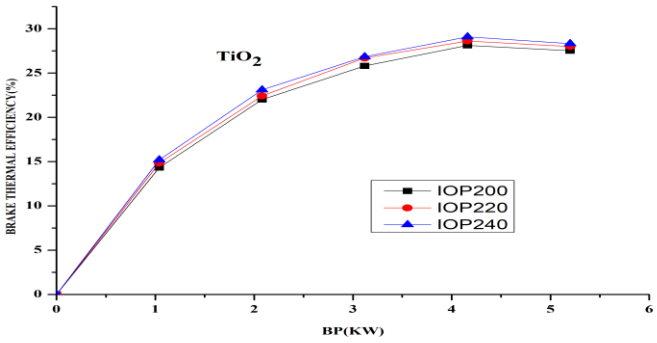

Figure 8: Deviation of BSFC vs BP for 20 and 100% blends of diesels.

This can be attributed to the high viscosity and low volatility of the blends, leading to inadequate atomization and mixture formation. The brake-specific fuel consumption (BSFC) for 100% biodiesel is higher compared to that of a 20% biodiesel blend. This is because 100% biodiesel possesses a lower heating value, necessitating excess fuel to maintain the engine's power output. Among the various diesel proportions, TIO2B20 exhibited a lower BSFC than other blends, closely resembling diesel fuel.

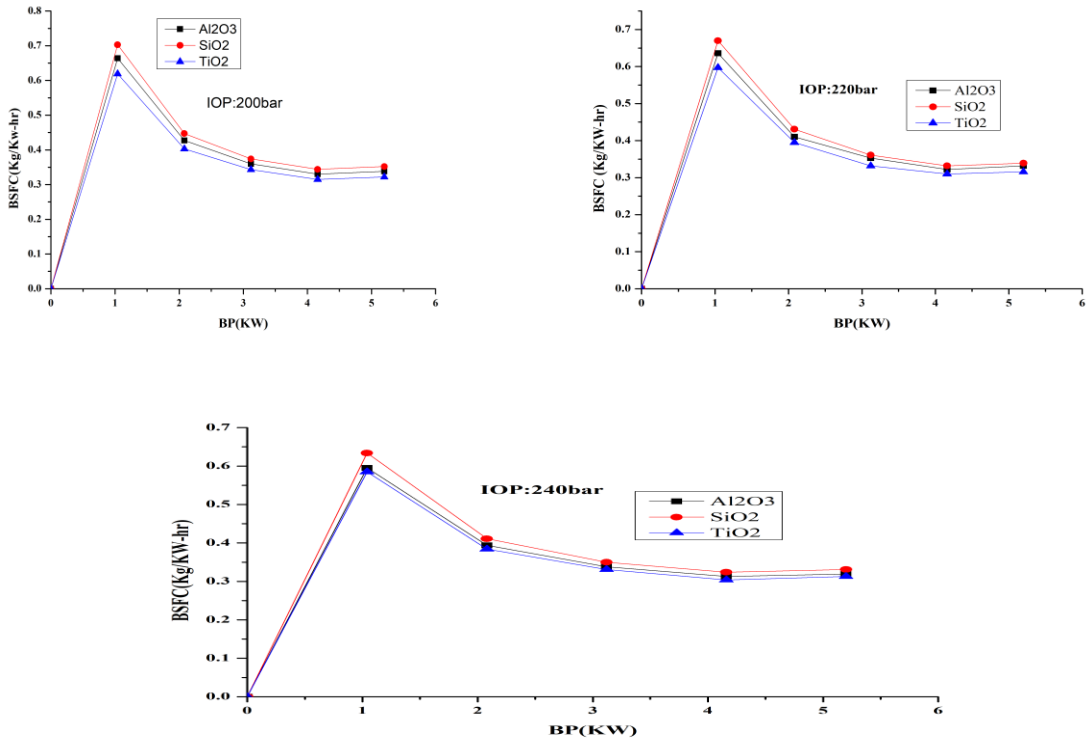

Figure 9: The Variation of BSFC with BP for various fuel blends

5.1.1.2. Brake Thermal Efficiency.

Figure 9 illustrates the variation of brake thermal efficiency (BTE) in relation to brake power (BP) for proportions of 20% and 100% of TiO_2, SiO_2, and Al_2O_3, as well as diesel. It is clear from the graph that diesel exhibited higher BTE. This could be attributed to the higher calorific value and lower density of diesel fuel.

Among the various proportions, B20 exhibited higher brake thermal efficiency (BTE) but lower than that of diesel. This is primarily attributed to factors such as calorific value (CV), cetane number, and density, which are nearly equivalent to diesel fuel. Additionally, from the graph, it is observed that 100% blends of the three biodiesels indicated lower BTE compared to 20% blends. This could be because the 20% blend possesses superior properties compared to 100% biodiesel.

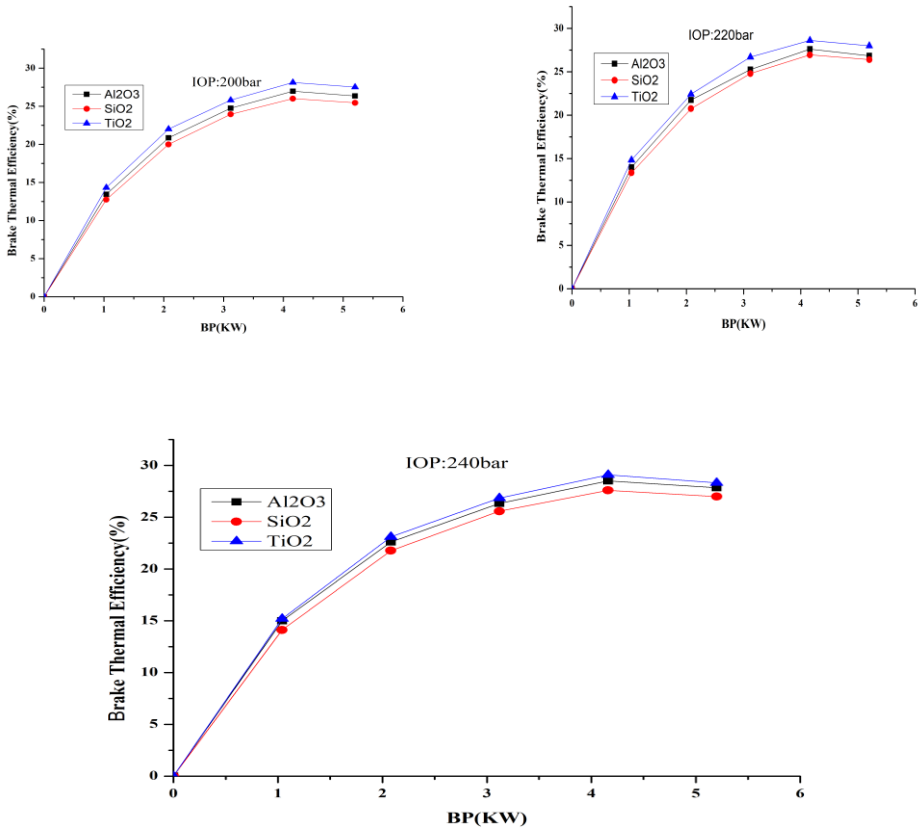

Figure 10: The variation of BTE with BP for various fuel blends

5.1.1.3. Exhaust Gas Temperature. The deviation of EGT concerning BP for 20 and 100% blends of TiO_2, Al_2O_3 and SiO_2, and diesel is shown in Figure 10. The EGT indicates

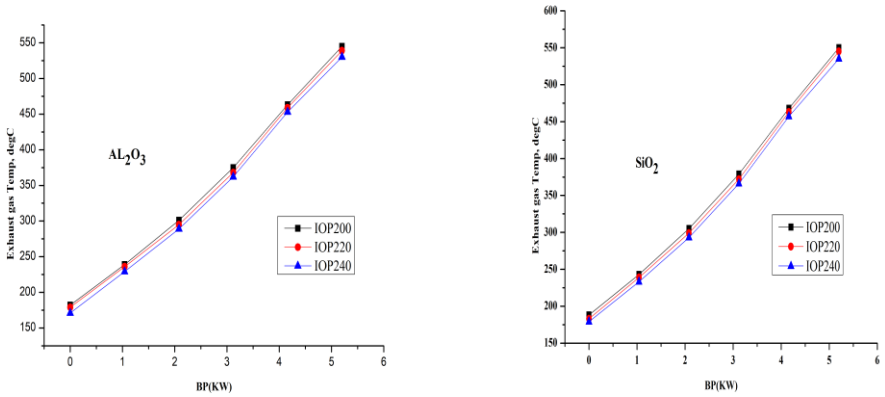

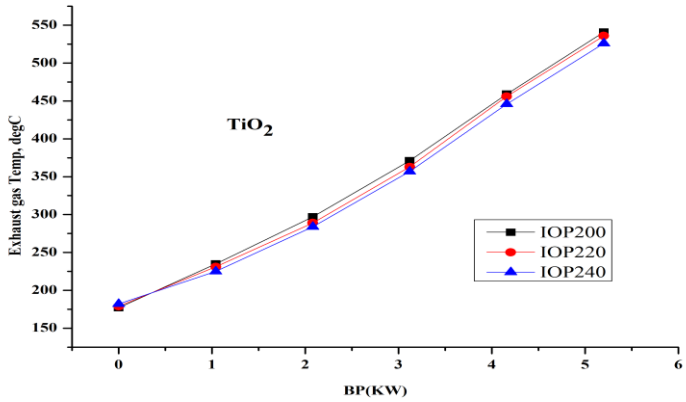

Figure 11: The variation of EGT with BP for various fuel blends

The fuel's heating capacity plays a significant role, with one-third of the heat being released as exhaust gas temperature (EGT). It is evident that EGT rises with increasing proportions of biodiesel across all loads. From the graph, it can be noted that B20 exhibited higher EGT compared to other blends at all loads. This could be attributed to B20's lower calorific value (CV) and higher density, resulting in incomplete combustion and thus elevating EGT. Additionally, B20 displayed lower EGT compared to the other blends, albeit with a slight increase over diesel. This is because B20 contains excess oxygen, higher CV, and lower density than other blends.

5.1.1.4. Carbon Monoxide Emission. Figure 11 illustrates the deviation of carbon monoxide (CO) emissions concerning brake power (BP) for proportions of 20% and 100% blends of TiO_2, Al_2O_3, and SiO_2, as well as diesel. It is evident from Figure 11 that MEMSO20 exhibits lower CO emissions, while diesel shows higher emissions across all loads. This suggests that biodiesel contains more oxygen, promoting complete combustion and improving combustion efficiency, thereby reducing CO emissions compared to diesel. The reduction in CO emissions for B20 can be attributed to the presence of excess oxygen and the effective combustion of biodiesel.

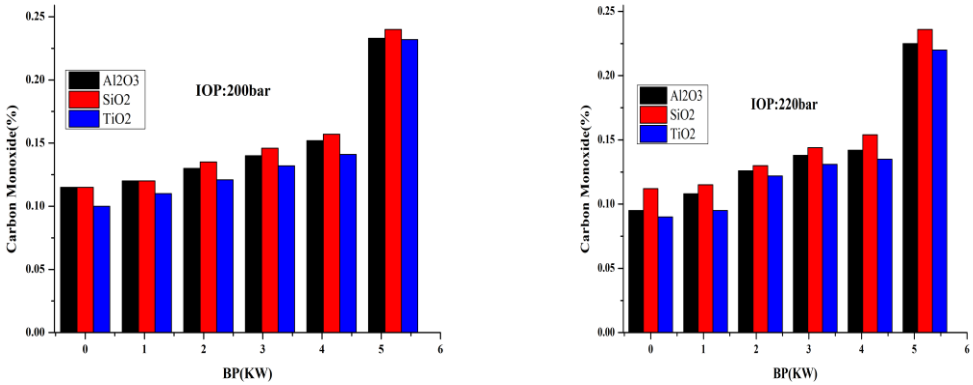

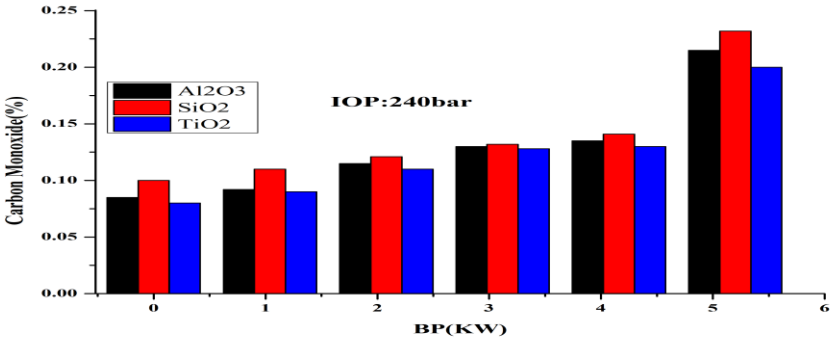

Figure 12: The variation of CO Emission with BP for various fuel blends

5.1.1.5. Hydrocarbon Emission. Figure 12 displays the deviation of hydrocarbon (HC) emissions concerning brake power (BP) for proportions of 20% and 100% blends of TiO_2, Al_2O_3, and SiO_2, as well as diesel. It is evident from Figure 12 that B20 exhibits lower HC emissions compared to other blend proportions and diesel across all load conditions.

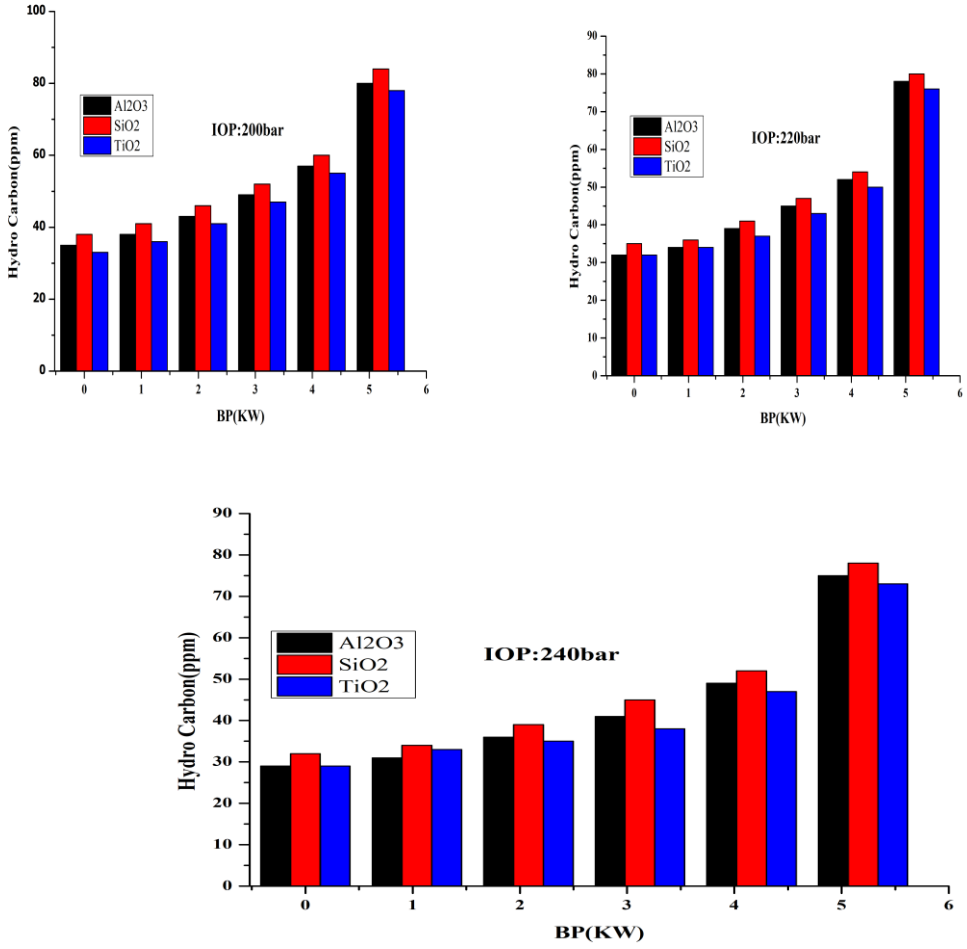

Figure 13: The variation of HC Emission with BP for various fuel blends

Due to its higher heating value, B20 results in more effective combustion. Among the different fuels, diesel exhibited higher HC emissions, possibly due to its lack of oxygen, resulting in poor atomization. It is observed that B40 shows higher HC emissions because it has a lower heating value compared to other blends.

5.1.1.6. Oxides of Nitrogen Emission.

Figure 13 illustrates the deviation of nitrogen oxide (NOx) emissions concerning brake power (BP) for proportions of 20% and 100% blends of TiO_2, Al_2O_3, and SiO_2, as well as diesel. The formation of NOx is influenced by the fuel's oxygen content, combustion flame temperature, and reaction time in the combustion chamber. NOx emissions from biodiesel blends are higher than those from diesel fuel and increase with load due to the higher combustion temperature and the presence of oxygen in biodiesel, resulting in higher NOx emissions compared to diesel fuel. SiO_2 exhibits lower NOx emissions compared to other blends among the different biodiesel blends.

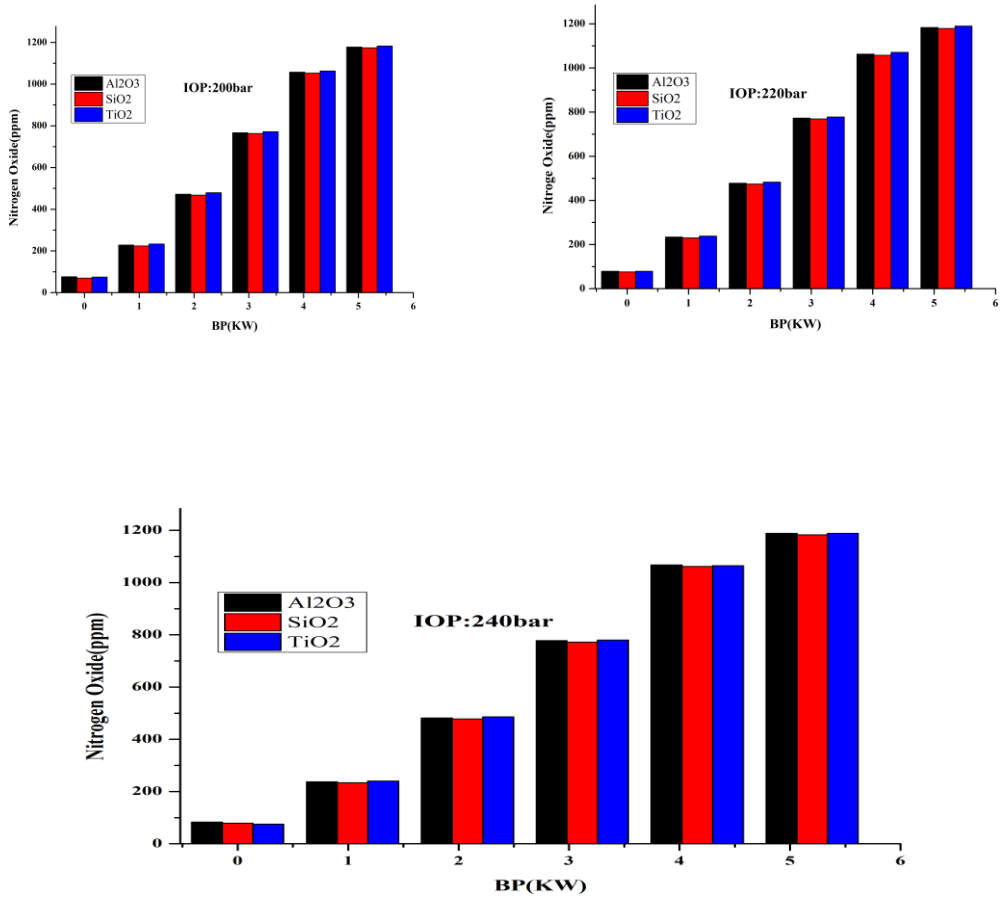

Figure 14: The variation of NOx with BP for various fuel blends

5.1.1.7. Smoke Opacity.

Figure 14 displays the variation in smoke opacity emissions concerning brake power (BP) for proportions of 20% and 100% blends of TiO_2, Al_2O_3, and SiO_2, as well as diesel. Smoke is primarily generated during the diffusive combustion phase.

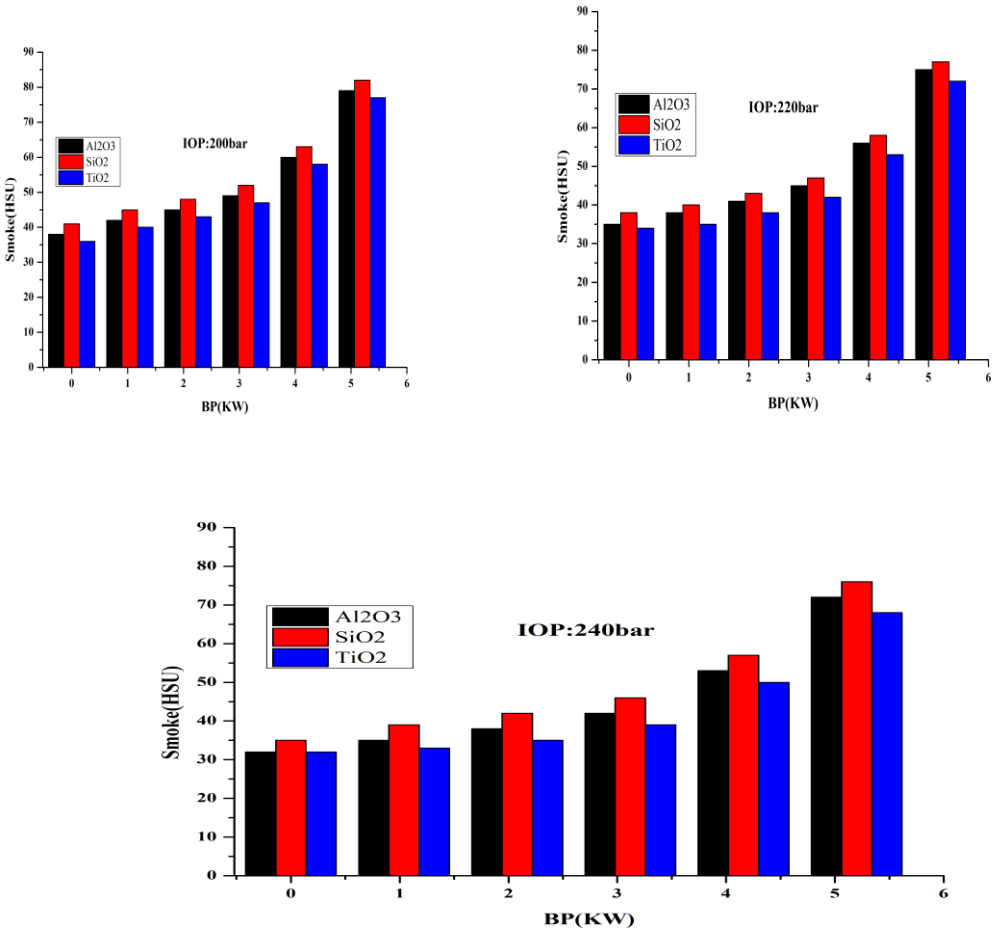

Figure 15: The variation of Smoke with BP for various fuel blend

As oxygenated fuel blends such as TiO_2, Al_2O_3, and SiO_2 contribute to enhancing diffusive combustion, it is observed from the graph that smoke opacity is lower for B40 across all loads. This is attributed to the higher heating value and excess oxygen in the fuel, promoting improved combustion and reducing smoke opacity. Among the biodiesel blends, B40 exhibited higher smoke opacity due to its lower heating value and cetane number, resulting in poorer combustion and increased smoke opacity. Additionally, the higher density of the 100% blend contributes to poor atomization. Diesel demonstrated higher smoke opacity due to the presence of aromatic compounds compared to biodiesel.

6. Conclusion

Different proportions of diesel blends and Jatropha oil with nano additives exhibit higher brake-specific fuel consumption (BSFC) than diesel fuel due to their high viscosity and volatility, resulting in poor atomization and mixture formation.

• 100% biodiesel blends demonstrate higher BSFC than 20% biodiesel blends due to their lower heating value, requiring excess fuel to maintain the same power output.

• Diesel fuel outperforms biodiesel blends in brake thermal efficiency (BTE) in all load conditions due to its higher calorific value and lower density.

• Among the biodiesel blends, B20 exhibits higher BTE but still lower than diesel due to comparable properties like calorific value, cetane number, and density.

• Exhaust gas temperature (EGT) increases with the proportion of biodiesel blends in all loads. B40 has higher EGT due to its lower calorific value and higher density, resulting in incomplete combustion.

• B20 demonstrates lower EGT than other blends but slightly higher than diesel due to its excess oxygen content, higher calorific value, and lower density.

• Carbon monoxide (CO) emissions are lower in all biodiesel blends, particularly B20, than diesel in all load conditions, indicating complete combustion and improved efficiency.

• Hydrocarbon (HC) emissions are lower in MEMSO20 than in other blends and diesel fuel at all loads, while diesel exhibits higher HC emissions due to a lack of oxygen and poor atomization.

• Nitrogen oxide (NOx) emissions are higher in biodiesel blends than diesel fuel in all loads due to the higher combustion temperature and the presence of oxygen. SiO_2 demonstrates lower NOx emissions compared to other blends.

• Smoke opacity is lower in B20TiO_2 at all loads than in other blends and diesel fuels due to a higher heating value and excess oxygen. B40TiO_2 shows higher smoke opacity in comparison due to its lower heating value and cetane number. Diesel fuel has higher smoke opacity due to aromatic compounds.

• Adding an additive like TiO_2, Al_2O_3, and SiO_2 to diesel fuel does not significantly affect BTE. Nano additives blends have higher BSFC than biodiesel fuel due to a slight power loss. Nano additives blend with 80ppm exhibits lower BSFC, suggesting more effective combustion.

Experimental findings reveal challenges associated with biodiesel blends exhibiting higher brake-specific fuel consumption (BSFC) and emissions, especially nitrogen oxides (NOx). Certain blend proportions, such as B40TiO_2, exhibit potential for enhanced performance and reduced emissions. The addition of antioxidant additives like LA may provide benefits such as

improved fuel stability. Further research and optimization efforts are necessary to enhance overall performance.

References

1) Ebrahimian, E.; Denayer, J. F. M.; Aghbashlo, M.; Tabatabaei, M.; Karimi, K. Biomethane and Biodiesel Production from Sunflower Crop: A Biorefinery Perspective. *Renewable Energy* 2022, *200*, 1352− 1361.
2) Elgharbawy, A. S.; Ali, R. M. Techno-Economic Assessment of the Biodiesel Production Using Natural Minerals Rocks as a Heterogeneous Catalyst via Conventional and Ultrasonic Techniques. *Renewable Energy* 2022, *191*, 161−175.
3) Mawlid, O. A.; Abdelhady, H. H.; El-Deab, M. S. Boosted Biodiesel Production from Waste Cooking Oil Using Novel SrO/ MgFe2O4Magnetic Nanocatalyst at Low Temperature: Optimization Process. *Energy Convers. Manag.* 2022, *273*, 116435.
4) Ashfaque Ahmed, S.; Soudagar, M. E. M.; Rahamathullah, I.; Sadhik Basha, J.; Yunus Khan, T. M.; Javed, S.; Elfasakhany, A.; Kalam, M. A. Investigation of Ternary Blends of Animal Fat Biodiesel- Diethyl Ether-Diesel Fuel on CMFIS-CI Engine Characteristics. *Fuel* 2023, *332*, 126200.
5) Saravanan, A.; Karishma, S.; Senthil Kumar, P.; Jayasree, R.Process Optimization and Kinetic Studies for the Production of Biodiesel from Artocarpus Heterophyllus Oil Using Modified Mixed Quail Waste Catalyst. *Fuel* 2022, *330*, 125644.
6) Yaashikaa, P. R.; Keerthana Devi, M.; Senthil Kumar, P.; Pandian, E. A review on biodiesel production by algal biomass: Outlook on lifecycle assessment and techno-economic analysis. *Fuel* 2022, *324*, 124774.
7) Nayab, R.; Imran, M.; Ramzan, M.; Tariq, M.; Taj, M. B.; Akhtar, M. N.; Iqbal, H. M. N. Sustainable Biodiesel Production via Catalytic and Non-Catalytic Transesterification of Feedstock Materials - A Review. *Fuel* 2022, *328*, 125254.
8) Wu, G.; Wang, X.; Abubakar, S.; Li, Y. A Skeletal Mechanism for Biodiesel-Dimethyl Ether Combustion in Engines. *Fuel* 2022, *325*, 124834.
9) Rajendran, N.; Kang, D.; Han, J.; Gurunathan, B. Process Optimization, Economic and Environmental Analysis of Biodiesel Production from Food Waste Using a Citrus Fruit Peel Biochar Catalyst. *J. Clean. Prod.* 2022, *365*, 132712.
10) Yahya, M.; Dutta, A.; Bouri, E.; Wadstrom, C.; Uddin, G. S. Dependence Structure between the International Crude Oil Market and the European Markets of Biodiesel and Rapeseed Oil. *Renewable Energy* 2022, *197*, 594−605.
11) Zhu, X.; Liu, S.; Wang, Z.; Zhang, Q.; Liu, H. Study of the Effect of Methanol/Biodiesel Fuel Mixtures on the Generation of Soot Particles and Their Oxidation Reactivity. *Fuel* 2023, *341*, 127632.
12) Maroušek, J.; Strunecký, O.; Bartoš, V.; Vochozka, M. Revisiting Competitiveness of Hydrogen and Algae Biodiesel. *Fuel* 2022, *328*, 125317.
13) Szulczyk, K. R.; Badeeb, R. A. Nontraditional Sources for Biodiesel Production in Malaysia: The Economic Evaluation of Hemp, Jatropha, and Kenaf Biodiesel. *Renewable Energy* 2022, *192*, 759−768.

14) Zhang, W.; Wang, C.; Luo, B.; He, P.; Zhang, L.; Wu, G.Efficient and Economic Transesterification of Waste Cooking Soybean Oil to Biodiesel Catalyzed by Outer Surface of ZSM-22 Supported Different Mo Catalyst. *Biomass Bioenergy* 2022, *167*, 106646.
15) Iyyappan, J.; Jayamuthunagai, J.; Bharathiraja, B.; Saravanaraj, A.; Praveen Kumar, R.; Balraj, S. Production of Biodiesel from Caulerpa Racemosa Oil Using Recombinant Pichia Pastoris Whole Cell Biocatalyst with Double Displayed over Expression of Candida Antartica Lipase. *Bioresour. Technol.* 2022, *363*, 127893.
16) (16) Zhang, X.; Li, N.; Wei, Z.; Dai, B.; Han, S. Synthesis and Evaluation of Bifunctional Polymeric Agent for Improving Cold Flow Properties and Oxidation Stability of Diesel-Biodiesel Blends. *Renewable Energy* 2022, *196*, 737−748.
17) Sharma, P.; Sharma, A. K.; Balakrishnan, D.; Manivannan, A.; Chia, W. Y.; Awasthi, M. K.; Show, P. L. Model-Prediction and Optimization of the Performance of a Biodiesel - Producer Gas Powered Dual-Fuel Engine. *Fuel* 2023, *348*, 128405.
18) Gohar Khan, S.; Hassan, M.; Anwar, M.; Zeshan; Masood Khan, U.; Zhao, C. Mussel Shell Based CaO Nano-Catalyst Doped with Praseodymium to Enhance Biodiesel Production from Castor Oil. *Fuel* 2022, *330*, 125480.
19) Uyumaz, A. Experimental Evaluation of Linseed Oil Biodiesel/ Diesel Fuel Blends on Combustion, Performance and Emission Characteristics in a DI Diesel Engine. *Fuel* 2020, *267*, 117150.
20) Yesilyurt, M. K. A Detailed Investigation on the Performance, Combustion, and Exhaust Emission Characteristics of a Diesel Engine Running on the Blend of Diesel Fuel, Biodiesel and 1-Heptanol (C7 Alcohol) as a next-Generation Higher Alcohol. *Fuel* 2020, *275*, 117893.
21) Longati, A. A.; Campani, G.; Furlan, F. F.; Giordano, R. d. C.;Miranda, E. A. Microbial Oil and Biodiesel Production in an Integrated Sugarcane Biorefinery: Techno-Economic and Life Cycle Assessment. *J. Clean. Prod.* 2022, *379*, 134487.
22) Sharma, V.; Kalam Hossain, A.; Ahmed, A.; Rezk, A. Study on Using Graphene and Graphite Nanoparticles as Fuel Additives inWaste Cooking Oil Biodiesel. *Fuel* 2022, *328*, 125270.
23) Mahmoud, A. H.; Hussein, M. Y.; Ibrahim, H. M.; Hanafy, M.H.; Salah, S. M.; El-Bassiony, G. M.; Abdelfattah, E. A. MixedMicroalgae-Food Waste Cake for Feeding of Hermetia Illucens Larvaein Characterizing the Produced Biodiesel. *Biomass Bioenergy* 2022,*165*, 106586.
24) Chen, Y.; Long, F.; Huang, Q.; Wang, K.; Jiang, J.; Chen, J.; Xu,J.; Nie, X. Biodiesel Production from Rhodosporidium Toruloides by Acidic Ionic Liquids Catalyzed Hydrothermal Liquefaction. *Bioresour.Technol.* 2022, *364*, 128038.
25) Gupta, R.; McRoberts, R.; Yu, Z.; Smith, C.; Sloan, W.; You, S.Life Cycle Assessment of Biodiesel Production from Rapeseed Oil:Influence of Process Parameters and Scale. *Bioresour. Technol.* 2022,*360*, 127532.

